Flow Field Characteristics of In-ground Stilling Basin Downstream of Flood Mitigation Dams

Mohammad. E. Meshkati Shahmirzadi
Dept. of Urban Management and Environmental Engineering, Kyoto Univ., Japan, E-mail: meshkati.ebrahim.65v@st.kyoto-u.ac.jp

Tetsuya Sumi
Disaster Prevention Research Institute, Kyoto University, Goka-sho, Uji-shi, 611-0011, Japan
E-mail: sumi.tetsuya.2s@kyoto-u.ac.jp

Sameh A. Kantoush
Civil Engineering Department, The German University in Cairo – GUC, New Cairo City, Main Entrance of Al-Tagamoa Al-Khames, Cairo – Egypt, E-mail: sameh.kantoush@guc.edu.eg

ABSTRACT: Flood mitigation dams (FMDs) in the normal condition permits the flow pass through the bottom outlet unobstructed. Meanwhile, a large percentage of river inflow can be temporarily stored within the reservoir during the flood events. Stilling basin, thus, is vital to dissipate the energy of outflow from FMDs to protect downstream reaches from unfavorable degradation and side bank erosions. However, the function of stilling basin in FMD is not only to dissipate the excess energy of the outflow, but also to let the sediment and fish pass through the structure unopposed. This paper introduces a new concept and design criteria to enhance the environmentally transparency of FMDs by In-ground Stilling Basin (ISB). The main objectives of the paper are: i) to clarify the flow field characteristics within the ISB and in the downstream; ii) to investigate the bed topography changes and assess flushing efficiency of flow and sediment through the ISB; and iii) to evaluate the interaction between sediment deposition and flow flied characteristics. To fulfill these objectives, the velocity profile, the water level fluctuations and flow visualizations have been monitored.

KEY WORDS: Flood Mitigation Dam, Hydraulic jump, Energy dissipation, Transparent dam, Flow field and sediment depositions.

1 INTRODUCTION

Floods are the most common natural hazards that human beings have faced in their history. Floods, especially those with greater frequency, can potentially lead to a catastrophic event. Overtime, the impact of floods on our life may be getting worse. This fact is mainly due to urbanization that creates a sharp growth in the value of properties and the number of infrastructure on flood plains. Human beings eventually cross the red-line of a healthy nature with such development. Automatically, the response of nature is intense and it causes much devastation and loss.

There are a wide range of methods and alternatives that have been suggested to provide flood protection. The main objectives of these methods are simply to reduce the inundation area of flood, resulting in the reduction of damage. These methods can be classified into two main categories: structural and non-structural measures. A Flood mitigation dam (FMD) maybe is the most effective structural measures designed only for the purpose of flood control. Different terminologies are given to FMDs worldwide e.g. in USA, an FMD is called a “Dry dam”, in Europe a “flood retention basin”, while in Japan it is called an “in stream flood control dam” (Kantoush and Sumi, 2010).

Apart from the different terminologies given to FMD, this kind of dam following a same strategy to reduce the impact of flood as in the normal river condition permits the flow to pass through the bottom outlet unobstructed.

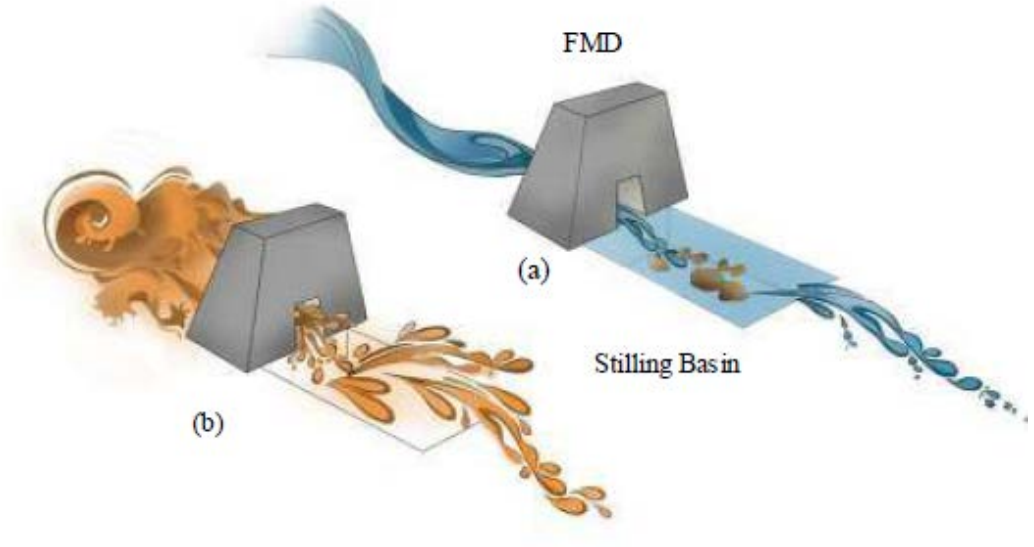

Figure 1 The schematic view of a FMD before (a) and during the flood event (b).

Meanwhile, a large percentage of river-inflow can be temporarily stored within the reservoir during the flood events (Lemperiere, 2006). The conceptual schematized view of FMD is shown in **Figure 1**. Apart from the retarded flood flow behind the flood mitigation dam, the excess flow is discharged through the dam's bottom outlet to the downstream river during flood events. The outflow form bottom outlet during flood is characterized by high velocity depending on the water elevation behind FMD. This high velocity could cause damage to the downstream areas if its energy is not dissipated well. A stilling basin, thus, is vital to dissipate the energy of outflow from FMDs by inducing hydraulic jumps (Bremen and Hager, 2000).

Although FMDs are considered eco-friendly, the design of FMDs is seriously facing three main challenges. These challenges are as follow: sediment deposition at the upstream area of FMDs, the bottom outlet and gate operation, and eco-friendly design of stilling basins (Sumi et al. 2011). Present paper is only focused on the design of stilling basin downstream of a FMD. In this regard, the main question is the optimal stilling basin geometry to maximize the energy dissipation, create easy passages for fish, sediment and minimize the cost.

The function of stilling basins in FMD, however, is not only to dissipate the excess energy of the outflow in flood events, but also to let sediment and aquatic species pass through the FMD unopposed during normal river conditions (Meshkati-Shahmirzadi and Sumi, 2013). There are several issues in the conventional design of stilling basins as follows: a) low energy dissipation efficiency; b) blocking fish migration and sediment supply, and c) high cost. Therefore, conventional stilling basins may not be adequate for the application to FMDs. In order to obtain the advantages of FMDs on sediment supply and fish migration, a careful design is required for stilling basins downstream of FMDs.

Tall and full width end-sill at the end downstream of stilling basin brings contradictory goals for FMDs. On the one hand, tall and full width end-sill can positively confine the hydraulic jumps within a limited area that finally lead to an economical design. On the other hand, tall full end-sill itself, indeed, is an obstacle against the fish migration and sediment transport. It negatively acts as an obstacle for sediment supply and fish migration; and also it would encourage the deposition of sediment within stilling basin that would build up over time in the stilling basin. The latter actually leads to a reduction in the design sequent depth that is required to trigger hydraulic jumps.

To reach the solution for the aforementioned problematic, a new concept of stilling basin was introduced; an in-ground stilling basin (ISB) in which the lower invert of a bottom outlet should be level

with the original river bed, so that the base flow in the river is able to pass through the bottom outlet unobstructed Figure 2. A further idea that has been investigated in this study is to consider free spaces at both sides of the end-sill, enabling there to be two free passes at the lateral sides of the channel, which could be an eco-friendly alternative for a common continuous end-sill.

Considerable number of studies, so far, has been dedicated to hydraulic jumps in non-prismatic stilling basin. Ohtsu and Yasuda (1990) investigated on jumps below an abrupt drop. Their experiments covered a wide range of step heights s/h_1 from 0.45 to 20 where s is the step height and h_1 is bottom outlet opening. They classified the drops into two main groups as follow: a) low drop: 0.5~1.5 $\leqslant s/h_1 \leqslant$8~9 and b) high drop: $s/h_1 \geqslant$15~16. For 9~10 $\leqslant s/h_1 \leqslant$14~15, which is called a medium drop, they could observe two different behaviors; if s/h_1 gets closer to 14~15 the flow pattern would be more similar to the high drop cases. On the contrary, if s/h_1 get smaller and close to 9~10 the flow pattern would be more similar to the low drop cases. For the s/h_1 less than 0.5 to 1.5, the flow condition is similar to the classical hydraulic jump in horizontal rectangular channels.

Larson (2004) recommended inducing forced hydraulic jumps to reduce the bottom outlet energy in culverts. In her study, she proposed two design layouts to induce a hydraulic jump within a culvert barrel: a) a rectangular full end-sill placed on flat apron of stilling basin and, b) a vertical drop along with a full end-sill. She found that both designs were operative in reduction of bottom outlet velocity as well as downstream scour. However, in her study she didn't consider the lateral enlargement and only focused on forced hydraulic jump below the drop.

Ohtsu et al. (1999) examined the stability of a submerged jump below the sudden lateral enlargement. They classified the submerged jump into three main flow patterns, steady asymmetric flow; asymmetric flow with periodic deflection; symmetric flow. They explored that the flow patterns is not only dependent on the upstream Froude number but also on the expansion ratio, $k=b_1/B$ where b_1 is the bottom outlet width, B is the width of stilling basin. The main outcomes of their study were providing series of equations to show the relations between hydraulic parameters (upstream Froude number, upstream approach flow depth) and geometrical parameters (expansion ratio k) with the jump sequent depth (h_2) and length (L_{sj}). Moreover, they presented an equation to obtain the minimum required sequent depth to obtain a stable and symmetric submerged jump downstream of a sudden enlargement. But they didn't force the jump to form at the vicinity of bottom outlet and instead they operate the flap gate far downstream of the channel. In their study they didn't deal with the drop.

Katakam and Rama (1988) introduced a new flow pattern below the simultaneous combination of an abrupt drop and sudden enlargement that they call a Spatial B-jump. The Spatial B-jump is a new flow pattern that contains the influence of both an abrupt drop and sudden lateral enlargement. The main variable parameters in their paper, were the upstream Froude number ranging from 2.2 to 6, the expansion ratio $k= b_1/B$=0.5 and 0.33, and the drop number $S=s/h_1$=0.4 to 6. They conclude that the sequent depth can be reduced by combining the sudden lateral enlargement and an abrupt drop.

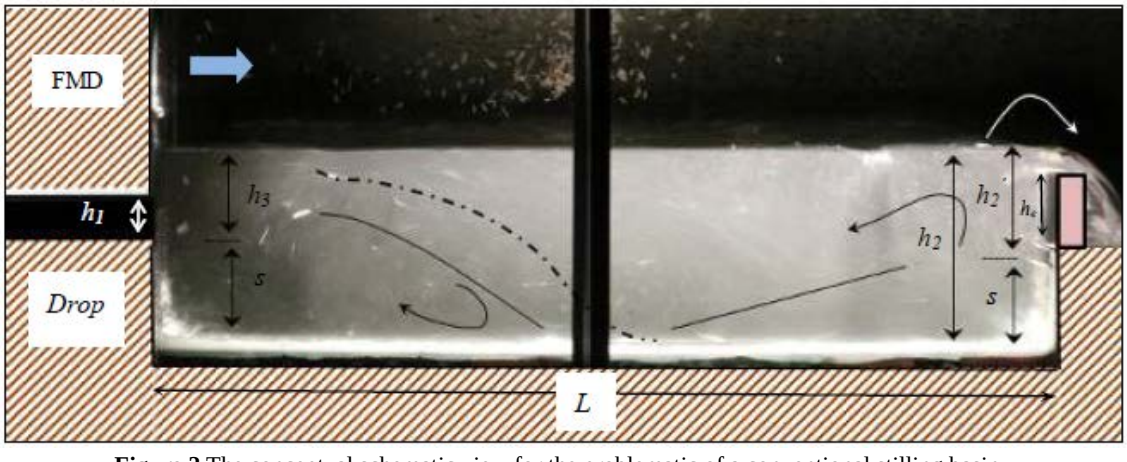

Figure 2 The conceptual schematic view for the problematic of a conventional stilling basin.

They also proposed two analytical equations for this type of jump. In their study, the influence of

end-sill to force the jump has not been considered.

Ferreri and Nassello (2002) studied the jumps that occur at a simultaneous combination of a sudden enlargement and abrupt drop in a rectangular channel. They found that, when the drop and enlargement are combined, as the depth of the downstream subcritical flow was increased various types of jumps are observed. They also stated that the characteristics of a certain jump type change with variation in the enlargement ratio of the upstream section, the initial Froude number and the relative drop height. In their study also, the effect of end-sill is not considered.

Based on the literature review it was found that, lack of enough information exist on the combination of a forced hydraulic jump with a simultaneous presence of a sudden enlargement and abrupt drop. Also, in FMDs usually one bottom outlet is located in the centerline and the width of the stilling basin is much wider than the width of the bottom outlet, which leads to a small expansion ratio, k, for the outflow. Ohtsu et al. (1999) noted the difficulties in forming stable hydraulic jumps with a small expansion ratio. Therefore, obtaining an optimal stilling basin in a way that provides us with all the advantages of FMDs as well as a stabilized hydraulic jump is a serious challenge. These facts motivated authors to conduct series of experiment intended to improve the design of SB for FMDs.

Moreover, due to the high turbulence and 3D nature of a hydraulic jump within an ISB, a robust design guideline for this structure is still lacking. Having a deeper evaluation and insight about the ISB mainly depends on a more accurate understanding of the flow pattern and behavior within this structure. These facts motivate the authors to conduct an experimental investigation on a number of proposal solutions. The major objectives of this paper are: a) To extend the knowledge on the 3D nature of hydraulic jump and its flow field characteristics within a complex geometry of ISB; b) To classify the flow patterns and propose a universal flow map for all possible patterns of flow within an ISB; c) To deeply clarify the effect of end-sill and free spaces at both sides of the end-sill on the performance of ISB. d) To inspect the performance of optimum (selected) ISB geometry in the presence of movable sediment. The results were tabulated in terms of statistical measures and also illustrated in the scatter plots.

2 MATERIALS AND METHODS

2.1 Model Setup

The experiments were conducted in hydraulic open laboratory of Kyoto University. The flume used to carry out the experiments was a 9 meter straight horizontal rectangular flume. The width and height of this flume was both equal to 50 cm. This flume had a transparent Plexiglas sidewall at its left side of stream flow direction that facilitates the visual access. The bottom outlet of main reservoir was faced to ISB; however its entrance was imitated from 50 cm inside of main reservoir. This guarantees the straight streamlines of flow discharge into ISB. Moreover, two pierced plates attached with pieces of cotton sheets were installed inside of main reservoir to attain the laminar flow before discharging out into the bottom outlet inlet. Then, the flow discharging out through bottom outlet was then uniform supercritical flow with a thickness equal to the bottom outlet.

A centrifugal pump was employed to support the recirculating water system by pumping up the water from underground sump tank into the upstream supply tank. The upstream supply tank was located at the upstream of the flume and equipped by a calibrated 90 degree V-notch weir. The 90 degree V-notch weir at the verge of upstream supply tank has been calibrated using average time-volume method for five reading for each flow rates. The flow finally flows out into ISB and there face to different configurations and geometries of ISB based on the test condition. Figure 4 shows the e schematic side and plan view of the physical model with the corresponding geometric parameters that have been considered in this paper.

2.2 Experimental Measurements and Observation

2.2.1 Hydraulic jumps properties

The basic data collection procedure was the same for all of the experiments run. The hydraulic jumps properties have been recorded mainly through visualization. However, during the experiments

notes also taken. For each test digital photographs were taken from side and top view of ISB. Moreover,

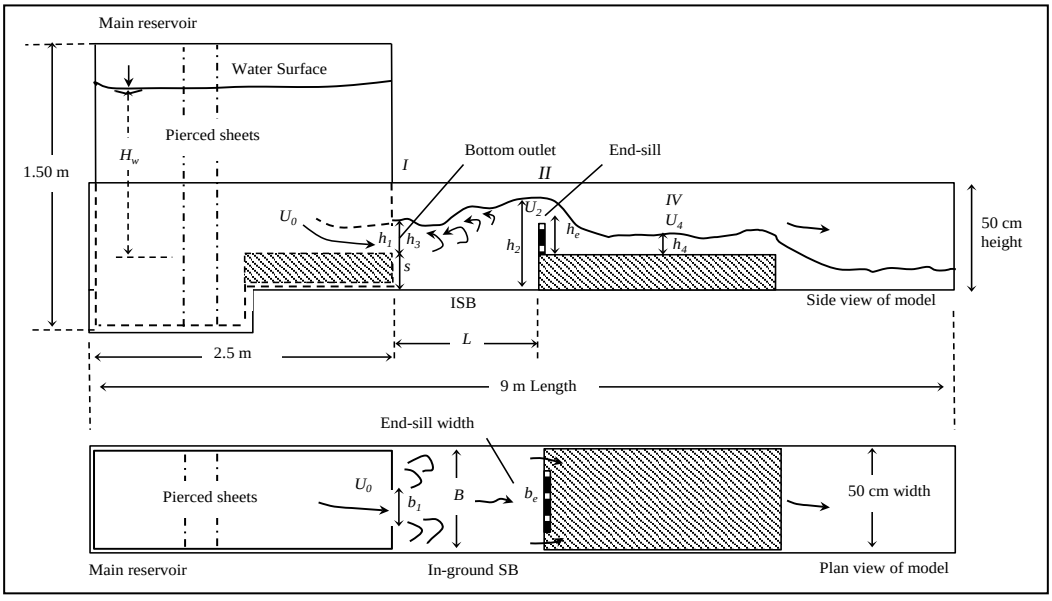

Figure 3 The schematic side and plan view of the constructed physical modal and the geometric and hydraulic parameters have been studied in this study.

using high resolution digital camera the flow condition has been recorded as movie. The electro-magnitude water level meter was used to measure the water depth and its fluctuation throughout ISB. Using an electro-magnetic current meter, the 3D components velocity was measured in different longitudinal and transversal cross sections. At every point the velocity was measured at 2.5 cm vertical interval. The sampling frequency was set to 50 H_Z.

2.2.2 Experimental condition

Figure 3 shows the schematic side and plan view of the constructed physical modal and the geometric and hydraulic parameters have been studied in this study. The experiments were carried out under different ISB geometries as follows: ISB length (L= 75, 100 and 125 cm), step depth (s= 5, 10 and 15 cm), however, the width of ISB for all experiments was the same B= 50 cm equal to the width of flume. For each ISB geometry configuration, different geometry of end-sill with various heights (h_e= 0, 4, 8 and 12 cm) has been systematically examined to obtain the optimum case. The end-sills were placed vertically above the positive step and perpendicular to the longitudinal axis of flume. In addition to the three different Froude number of supercritical flow at the bottom outlet (namely $Fr_1=U_0/(gh_1)^{0.5}$=2.8, 4.9 and 5.1), only one dimension of bottom outlet (h_1= 5 cm and b_1= 10 cm) was examined, thus, creates an expansion ratio of k=0.2 ($k=b_1/B$).

3 RESULTS AND DISCUSSION

3.1 Evaluation of Flow Patterns and Stability of the Jump

Depending on the geometry of ISB, five different jump types have been observed: B-jump, S-jump, U-jump, periodic submerged jump and steady submerged jump (Figure 4(a)-(d)). The detail explanations about characteristics of jump types within ISB are given in Meshkati-Shahmirzadi and Sumi (2013). For sake of brevity, only the main points are described herein. For Froude number ranged from 2.5 to 5.5, the types of hydraulic jumps were less dependent on Fr_1, and more dependent on the end-sill height h_e. For an ISB without end-sill, the B-jump and S-jump are the most possible flow patterns to be initiated within ISB. For a medium height of end-sill the S-jump and U-jump have been more often observed. Taller end-sills in general provide a steady submerged jump within ISB. For a given height of end-sill and

Froude number with longer increasing ISB length of negatively induced the periodic an oscillation of the flow. However, the compact and deep ISB perfectly stabilized the flow.

(a) **(b)** **(c)** **(d)**

Figure 4 Four different jump types that have been initiated within ISB under different hydraulic and geometric conditions (a) B-jump; (b) U-jump; (c) Periodic submerged jump; (d) Steady submerged jump.

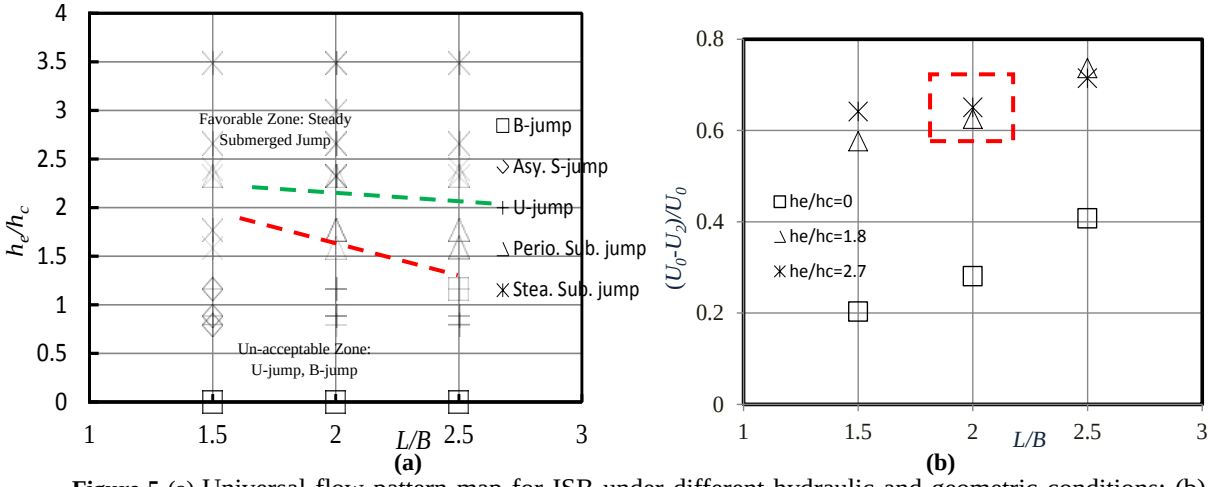

Figure 5 (a) Universal flow pattern map for ISB under different hydraulic and geometric conditions; (b) Velocity reductions within ISB versus the normalized length of ISB.

3.2 Proposing a Universal Flow Patterns Map for ISB

Using successful experimental data, a universal flow pattern map is proposed in Figure 5(a). This figure has been made based on the wide range of hydraulic and geometrical parameters that described in section 2.3. The horizontal axis represents the aspect ratio of ISB, *L*/*B*, and the vertical axis is the normalized height of end-sill. All five possible hydraulic jumps types are shown in this flow pattern map. This flow pattern map provides three zones of favorable, acceptable and un-acceptable geometry of ISB. The favorable zone is representative of the steady submerged flow, the upper area from the green line. The area between green and red line is called acceptable zone in which the periodic submerged flow happens. The area below the red line is un-acceptable geometry for ISB. In this zone, the energy dissipation is insufficient where the flow pattern is mostly periodic and sometimes asymmetric.

3.3 The Effect of Length on ISB Performance

Figure 5(b) shows the effect of normalized ISB length on normalized velocity reduction at centerline of ISB and in stream-wise direction. U_0 is the flow velocity at the face of bottom outlet that is called section *I*; and U_2 is the maximum average velocity just upstream of end-sill. This figure illustrates the ISB performance regarding to velocity reduction consistently enhanced by increasing the ISB length, in

particular in case of lower end-sill height e. g. h_e/h_c=0. Since the slope rate of velocity reduction is milder compare to the case without end-sill. Therefore, by considering a taller end-sill we could reduce the ISB length. Reduction of ISB length is cost efficient. Thus, considering the economical aspect in design, maybe the normalized ISB length equal to 2 (L/B=2) may be an optimum length.

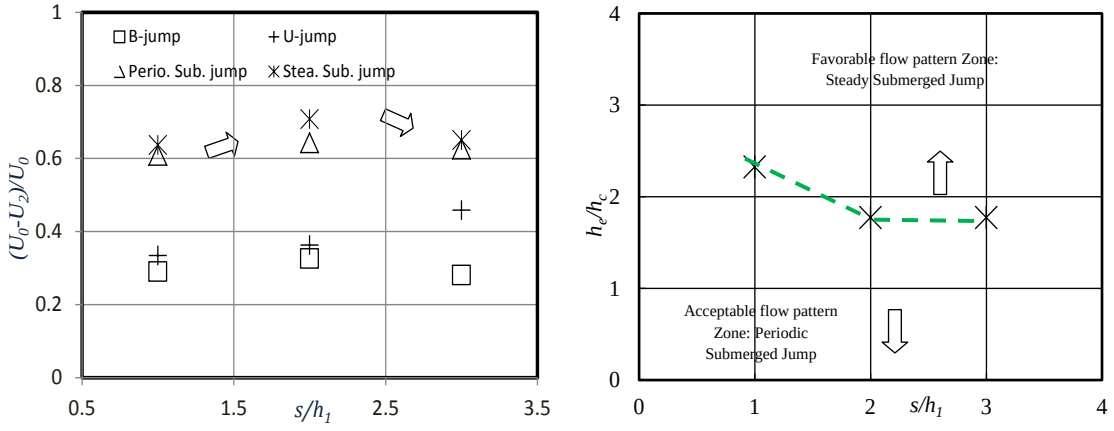

(a) **(b)**

Figure 6 (a) Velocity reduction within ISB versus drop number s/h_1; (b) the boarder of favorable flow pattern and acceptable flow pattern for different drop numbers along with ISB.

3.4 The Effect of Depth on ISB Performance

The effect of drop number s/h_1 has been studied in present paper. Based on the classification of Ohtsu and Yasuda (1990) on drop types, which is earlier mentioned, the drop numbers here in this study are known as low drop, 0.5~1.5 $\leqslant s/h_1 \leqslant$8~9. Figure 6(a) depicts the normalized velocity reduction within ISB for different drop numbers and various hydraulic jump types. The horizontal axis in Figure 6(a) is drop number and the vertical axis is the normalized velocity reduction. Increasing the drop number, it didn't show a significant effect on the performances of ISB. However, for taller end-sills, when the jump types are submerged, there is an optimum value for ISB length in which the maximum velocity reduction obtained, s/h_1= 2.

Figure 6(b) attempts to show the boarder of favorable flow pattern zone influenced by drop number. When drop number increased; a shorter end-sill for ISB can provide a favorable flow pattern (steady submerged jump). Whereas further increase in ISB depth, it didn't permit us to further shorten the end-sill height. Therefore, an optimum depth to satisfy both higher velocity reduction and economical aspect is s/h_1=2.

3.5 The Effect of End-sill Height and Free Spaces on ISB Performance

To identify the effect of end-sill height on performance of ISB, four tests were designed in which all parameters were constant and only the end-sill height varied (Table 1). In order to investigate the effectiveness of different ISB geometry in flow velocity reduction, the normal stream-wise velocity (U_{max}/U_0) along the centerline of ISB is plotted against the normal distance from the bottom outlet section (x/L). U_{max} is the maximum average velocity in each profile along the centerline of ISB. Figure 7(a) plots the normalized velocity reduction under different end-sill heights. In case of experiment without end-sill (EH1), the U_{max}/U_0 was remained considerably high until the end of ISB. While for the cases EH3 and EH4, respectively 8 and 12 cm end-sill height the lowest magnitude of U_{max}/U_0 was observed at the end of ISB. Additionally, this figure indicates that increasing the height of end-sill from 8 to 12 cm (EH3 to EH4) did not enhance the performance of ISB regarding to velocity reduction. Then, it can be conclude that a taller end-sill could dissipate more energy than the lower, however increasing the end-sill height above an optimum value caused no enhance in the performance of ISB. The normalized end-sill height, h_e/h_c, greater than 2 can provide an acceptable velocity reduction around 60 to 70% within ISB. Figure 8(a) shows the normalized velocity reduction within ISB versus the normalized end-sill height under different

drop numbers. This figure evidences that further increase in end-sill height did not show always a better velocity reduction.

To clarify the effect of free spaces (end-sill width) on velocity reduction along the ISB, three tests herein were presented in which all parameters were constant and only the end-sill width varied. The designed geometric and hydraulic variables of tests are tabulated in Table 1 (EW1, EW2 and EW3). Figure 7(b) illustrates the normal stream-wise velocity (U_{max}/U_0) reduction against the normalized distance from the bottom outlet section (x/L) for 8 cm height of end-sill under different free spaces. Considering two free spaces at the both side of end-sill slightly reduced the performance of ISB for velocity reduction; however the magnitude of (U_{max}/U_0) did not change considerably. Thus, free spaces in addition to facilitating the fish and sediment passage has not significant impact on ISB performance.

3.6 Flow Condition Downstream of ISB

Figure 8(b) illustrates the normalized velocity reduction between section I and IV (downstream of ISB). U_4 is the average velocity of flow at section IV. The overall trend of data plotted in this figure shows by increasing the normalized height of end-sill the normalized velocity reduction is reducing. In other words, in contrary with the necessity of taller end-sill to create a steady submerged jump within a confined space, the taller end-sills negatively reproduce the higher flow velocities at ISB downstream. Then a medium height of end-sill can guarantee a better condition for flow filed downstream of ISB. The red box at Figure 8(b) shows the optimum range for normalized end-sill height. Thus, in case of submerged jumps within ISB, the best normalized end-sill height, h_e/h_c, to create an acceptable downstream condition ranged from 2 to 3.

Table 1 The designed geometric and hydraulic variables to investigate the effect of height and free spaces at both sides of end-sill.

Case	Q (lit/sec)	Fr_1	h_1 (cm)	b_1 (cm)	L (cm)	s (cm)	h_e (cm)	b_e (cm)
EH1	15	4.3	5	10	100	15	0	50
EH2	15	4.3	5	10	100	15	4	50
EH3	15	4.3	5	10	100	15	8	50
EH4	15	4.3	5	10	100	15	12	50
EW1	15	4.3	5	10	100	15	8	50
EW2	15	4.3	5	10	100	15	8	40
EW3	15	4.3	5	10	100	15	8	30

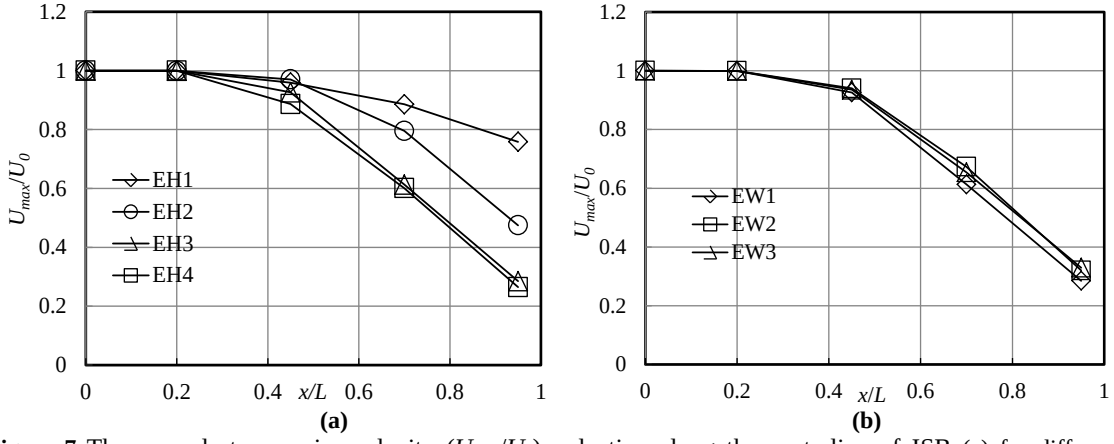

Figure 7 The normal stream-wise velocity (U_{max}/U_0) reduction along the centerline of ISB (a) for different end-sill height h_e and (b) different end-sill width b_e.

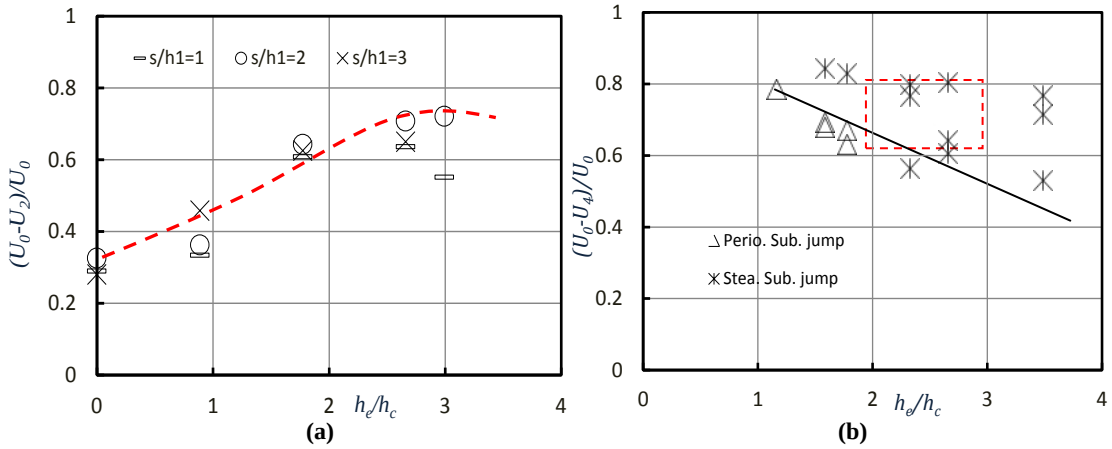

Figure 8 (a) The normalized velocity reduction between section *I* and *II* versus h_e/h_c; (b) Normalized velocity reductions between sections *I* and *IV* versus h_e/h_c.

3.7 Evaluation of ISB Performance in Presence of Movable Sediment

To inspect the performance of selected ISB geometries in the presence of movable sediment, eight experiments were designed as shown in Table 2. The experimental conditions consist of two grain sizes of sediment; sand with diameter of 3 mm and gravel with diameter of 15 mm, each spread flat over the apron of the ISB to explore the effect of the sediment on the flow pattern and energy dissipation function in the ISB. Both the sand and gravel used in this study was uniform and non-cohesive.

The experiments carried out with sand are named SS1-4. The ISB was filled with sand with a thickness of 10 cm and each test was run for 2 hours to reach the equilibrium condition. It was found that, the flushing efficiency of ISB in presence of movable sediment with 3 mm diameter is very high and it is difficult to obtain equilibrium condition. The majority of sediment was washed out from the ISB. Furthermore, in the experimental cases with two free spaces at both sides of the end-sill (SS2 and SS4), the removal process was made even faster. Due to high rate of sediment flushing, the sediment deposition within the ISB after equilibrium was negligible. That is why the stream-wise velocity profile for the clear water condition (blue line) and movable bed condition in equilibrium (red line) are almost identical (Figure 9).

Table 2 The designed geometric and hydraulic variables to investigate the effect of height of end-sill and its free spaces in presence of sediment within ISB.

Case	Q (lit/sec)	Fr_1	h_1 (cm)	b_1 (cm)	L (cm)	s (cm)	h_e (cm)	b_e (cm)	d_{50} (mm)
SS1	15	4.3	5	10	100	10	8	50	3
SS2	15	4.3	5	10	100	10	8	40	3
SS3	15	4.3	5	10	100	10	12	50	3
SS4	15	4.3	5	10	100	10	12	40	3
SG1	15	4.3	5	10	100	10	8	50	15
SG2	15	4.3	5	10	100	10	8	40	15
SG3	15	4.3	5	10	100	10	12	50	15
SG4	15	4.3	5	10	100	10	12	40	15

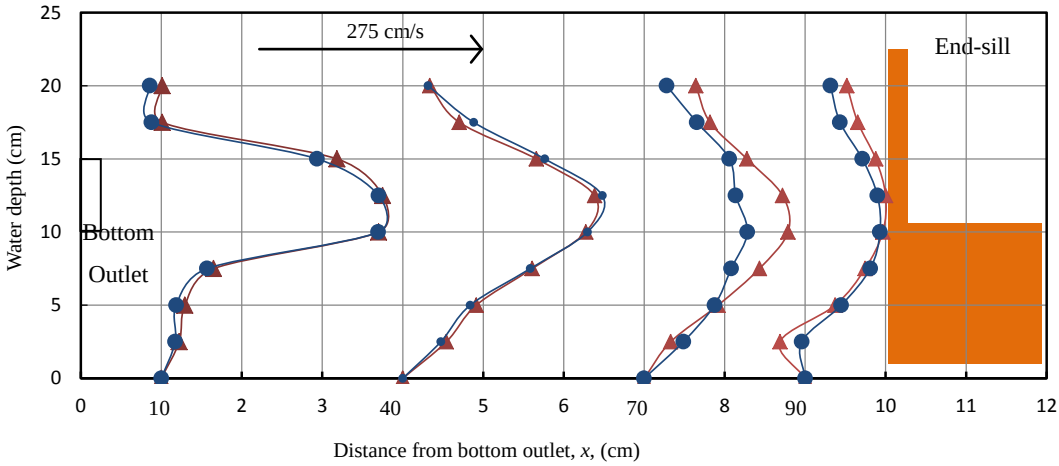

Figure 9 The stream-wise velocity profile for clear water condition (blue line) and movable bed condition in equilibrium (red line), h_e=12, b_e=50, Q=15 l/s.

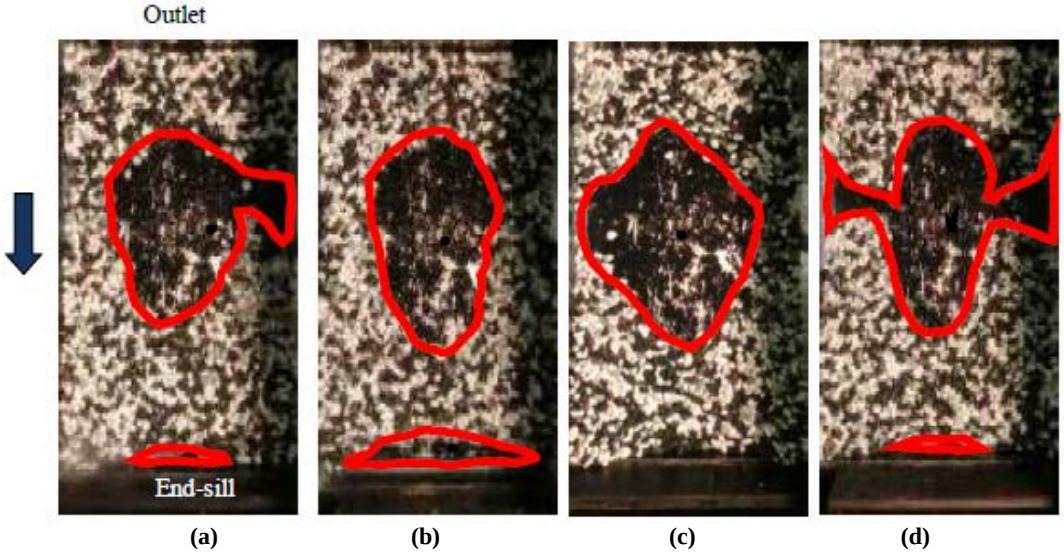

Figure 10 The bed topography in equilibrium condition within ISB, d_{50}=15 mm, (a) h_e= 8 cm, b_e= 50 cm; (b) h_e= 8 cm, b_e= 40 cm; (c) h_e= 12 cm, b_e= 50 cm; (d) h_e= 12 cm, b_e= 40 cm.

The second series of experiments were performed using gravel. These experiments are named SG1-4 in Table 2. The main objective of these experiments was to understand both the flushing (self-cleaning) efficiency of the ISB and also the area within the ISB that may not need extra protection to avoid wear. The gravels with a mean diameter of 15 mm were spread over the apron of the ISB with 3 cm thickness. The experiments were conducted for 2 hours. Figure 10(a) to (d) illustrates the final bed topography within the ISB. It was found that, having free spaces at both sides of end-sill resulted in a symmetric bed topography as shown in Figure 10(b). While, in case of no free spaces, the bed topography in the equilibrium state was asymmetric. Interestingly, the taller end-sill provided a better performance in terms of flushing efficiency (the scoured area highlighted by red lines in Figure 10). For the end-sill height equal to 8 cm, both with and without free spaces, almost no sediment was flushed out from the ISB. This fact negatively reduced the ISB's performance regarding energy dissipation and velocity reduction. In this case the formation of a U-jump was observed within the ISB, while in the presence of no sediment, the jump type ranged between a steady submerged jump and a periodic submerged jump.

3.8 Conclusion

To provide a higher chance for sediment supply and fish migration through the FMD, it has been suggested by previous studies made by the authors to consider a drop below the bottom outlet extending to the downstream end of the stilling basin. This consideration would create a stilling basin where its geometry is similar to a pool, called an in-ground stilling basin (ISB). Amongst different types of jump possibilities within the ISB, this study pays close attention to the steady submerged hydraulic jump. The velocity reduction of the stream-wise flow affected by different end-sill heights and widths was experimentally investigated and the following results were concluded:

1- The taller end-sill can effectively reduce the magnitude of velocity within the ISB compared to shorter end-sill.

2- Although the presence of a tall end-sill at the downstream end of the ISB could stabilize the hydraulic jump, a taller end-sill negatively accelerated the downstream velocity due to the free fall flow over the end-sill.

3- Considering two free spaces at the lateral sides of end-sill (slit-type) shows almost an equal function for velocity reduction compared with an end-sill without free spaces and positively provides additional effects for fish and sediment passing.

4- Considering a medium drop number of the ISB can positively improve the velocity reduction, while further increasing the depth showed no benefit in either velocity reduction or construction cost.

5- The flow pattern within the ISB was depends more on the end-sill height rather than the variation in the upstream hydraulic condition (e.g. Froude number). Moreover, it was found that increasing the length of the ISB decreased the stability of flow.

6- The optimum geometry of the ISB was found to be as follows: $2<h_e/h_c<3$, $s/h_1=2$ and $L/B=2$, for the Froude number range between 2.8 and 5.1.

7- Both the taller end-sill and free spaces can positively improve the self-cleaning process within the ISB. Furthermore, free spaces can provide a stable symmetric flow pattern within the ISB by artificially reducing the expansion ratio.

References

Bremen, R., and Hager, W.H., 1993. T-jump in abruptly expanding channel, J. of Hydraulic Research, IAHR, Vol.31,pp.61–78. Chow, V.T., 1959. Open channel hydraulics", McGraw-Hill, New York.

Ferreri, G.B., and Nasello, C., 2002. Hydraulic Jumps at Drop and Abrupt Enlargement in Rectangular Channel, J. Hydraul. Res. Vol.40, pp. 491–505.

Kantoush, S.A., Sumi, T., 2010. Influence of stilling basin geometry on flow pattern and sediment transport at flood mitigation dams, Proc. of 2nd Joint Federal Interagency Conference, Las Vegas, USA.

Katakam, V.S.R., Rama, P., 1998. Spatial B-jump at sudden channel enlargements with abrupt drop, J. of hydraulic engineering, Vol.124, pp.643-646.

Larson, E. A., 2004. Energy dissipation in culverts by forcing a hydraulic jump at the outlet, Thesis on Master of Science in civil engineering, Washington state University.

Lempérière, F., 2006. The role of dams in the XXI century, Achieving a sustainable development target, Hydropower and Dams, Issue Three, pp. 99-108.

Meshkati Shahmirzadi, M. E., and Sumi, T., 2013. Hydraulic Design of In-ground Stilling Basin under Submerged Jump Condition in Flood Mitigation Dams, J. of Japan Society of Civil Engineering, Vol. 69, pp. 79-84.

Ohtsu, I., Yasuda, Y., and Awazu, S., 1990. Free and submerged hydraulic jump in rectangular channels", Report No. 35, Res. Inst. of Sci. and Tech., Nihon Univ., Tokyo, Japan.

Ohtsu, I., Yasuda, Y., and Ishikawa, M., 1999. Submerged hydraulic jumps below abrupt expansions, J. of Hydraulic Engineering, ASCE, Vol. 125, pp. 492–499.

Sumi, T., Kantoush, S. A., and Shirai, A., 2011. Worldwide Flood Mitigation Dams: Operating and Designing Issues, the international symposium on urban flood risk management, 21-23 September, 2011, Graz, Austria.